

Observation and Mechanism of Collision-Induced Desorption: CH₄ on Ni(111)

J. D. Beckerle, A. D. Johnson, and S. T. Ceyer^(a)

Department of Chemistry, Massachusetts Institute of Technology, Cambridge, Massachusetts 02139

(Received 19 September 1988)

The desorption of CH₄ physisorbed on Ni(111) is observed to be induced by collision with Ar atoms incident with energies less than 2 eV. The absolute cross section for collision-induced desorption is measured as a function of the kinetic energy and incident angle of the Ar beam. The mechanism for desorption is shown to involve a direct and impulsive, bimolecular collision between Ar and CH₄. Molecular-dynamics simulations show that the energy and incident-angle dependence of the desorption cross section are the consequence of two competing dynamical effects.

PACS numbers: 82.65.Pa, 34.50.Bw

Desorption induced by an energetic beam of particles is not a novel phenomenon. Argon-ion-sputtering, secondary-ion, and fast-atom-bombardment mass spectroscopy employ this process as a means to vaporize solids for the purpose of removing adsorbed contaminants, depth profiling, or producing a source of ions for mass spectrometric analysis. However, the energies of the incident particles are typically orders of magnitude greater than the adsorbate binding energies, resulting not only in desorption of the adsorbate but also in massive substrate desorption via a collision cascade in the hot spot induced by the incident particle.^{1,2} In contrast to these invasive interactions, we report that the desorption of the adsorbate only can be induced by a direct, bimolecular collision with an incident neutral atom whose energy is equal to or slightly above the threshold energy for desorption.³ Specifically, we have measured the absolute cross section for desorption of CH₄ physisorbed on Ni(111) induced by collision with an incident Ar atom as a function of the energy and incident angle of the Ar atom. With the aid of classical molecular-dynamics simulations, the mechanism for collision-induced desorption is established and the complicated dependence of the cross section on the Ar kinetic energy and incident angle is shown to be the result of two competing dynamical effects.

The cross sections are measured in an apparatus previously described in detail.⁴⁻⁷ Briefly, the apparatus consists of a supersonic molecular beam source precisely coupled to a UHV main chamber equipped for surface analysis. Monoenergetic Ar-atom beams with kinetic energy up to 51.8 kcal mol⁻¹, as measured by a time-of-flight technique, are generated by expanding a mixture of 1% Ar seeded in He from a variable-temperature nozzle. The Ni(111) single-crystal surface is mounted on a liquid-He-cooled manipulator.⁸ The diameter of the molecular beam at the crystal position is slightly larger than the crystal so that the entire surface is exposed to the beam for all incident angles. The procedures for cleaning the crystal and for analysis of its composition are as described previously.^{4,5}

The experimental procedure for the study of collision-induced desorption is similar to that of a thermal-desorption measurement. Molecular CH₄ is physisorbed onto the entire Ni(111) surface at 40 K. The surface is subsequently exposed to a monoenergetic Ar beam of known flux, kinetic energy, and angle of incidence, while the time-dependent partial pressure of CH₄ evolving from the surface as a result of collision-induced desorption is monitored using a quadrupole mass spectrometer. Under the conditions of a desorption measurement, no carbon resulting from collision-induced dissociative chemisorption⁹ is observed on the surface.

As in thermal-desorption measurements, the partial-pressure change is directly proportional to the instantaneous rate of collision-induced desorption of CH₄ from the surface, $-d\theta_{\text{CH}_4}/dt$. The cross section for collision-induced desorption Σ_D is calculated from the relation

$$-d\theta_{\text{CH}_4}/dt = \Sigma_D(E_i, \theta_i, \theta_{\text{CH}_4}) F_S \theta_{\text{CH}_4}(t),$$

where E_i and θ_i are the kinetic energy and angle of incidence of the Ar atoms and θ_{CH_4} is the coverage of CH₄. The quantity F_S is the number of Ar atoms that strike the surface per unit surface area per unit time and is equal to the absolute flux of the Ar-atom beam measured perpendicular to the beam axis, F_B , multiplied by a factor of $\cos\theta_i$. With this definition for the incident beam flux, Σ_D is the *surface area* in which an Ar-atom impact yields a desorption event per physisorbed CH₄ molecule.

The results for Σ_D as a function of θ_i are plotted in Fig. 1 for a range of E_i . The open symbols correspond to measurements performed at very low CH₄ coverage, less than 0.01 monolayer, to avoid the presence of islands of physisorbed CH₄.¹⁰ Therefore, these desorption cross sections correspond to an Ar atom interacting with an isolated CH₄. The filled symbols in Fig. 1 are Σ_D measured at a saturation CH₄ coverage of 0.33 monolayer as established by LEED measurements¹⁰ and shown at the normal angle only. The absolute magnitudes of Σ_D at normal incidence for both the isolated CH₄-molecule limit and the saturated monolayer coverage are identical.

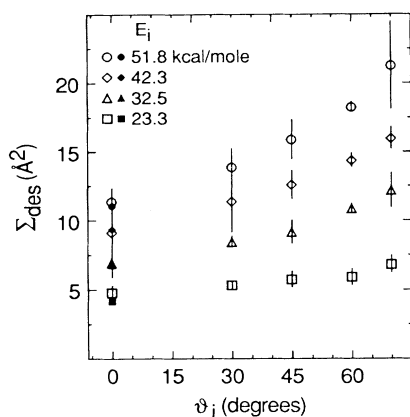


FIG. 1. Absolute cross sections for collision-induced desorption Σ_D as a function of the Ar angle of incidence and kinetic energy. The error bars are statistical 95%-confidence limits for a series of three to four measurements for each data point. The open points represent measurements made for $\theta_{\text{CH}_4} \leq 0.01$ monolayer. The filled points at $\theta_i = 0^\circ$ represent measurements made for $\theta_{\text{CH}_4} = 0.33$ monolayer.

This is an important observation because it indicates that indirect, surface-mediated processes which would result in desorption of multiple CH_4 molecules from a single Ar-atom impact at saturation coverage do not contribute significantly to the desorption mechanism. It is therefore concluded that the dominant mechanism of collision-induced desorption at low CH_4 coverage involves the direct, bimolecular collision of the incident Ar with the physisorbed CH_4 . This conclusion is further supported by the small magnitude of Σ_D at normal incidence, 11.4 \AA^2 , compared to the Ar- CH_4 hard-sphere collision cross section of approximately 30 \AA^2 .

As shown in Fig. 1, Σ_D measured at low coverage exhibits a complex dependence on θ_i . At $E_i = 51.8 \text{ kcal mol}^{-1}$, the Σ_D doubles as θ_i is increased from 0° to 70° , while at $23.3 \text{ kcal mol}^{-1}$, it is almost independent of θ_i . With the intent of uncovering the physical origin of these trends, we have performed three-dimensional, classical trajectory calculations on a simple model. The details of the calculation are described elsewhere.¹⁰ In the model, Ar and CH_4 are treated as hard spheres with diameters of 2.8 and 3.2 \AA , respectively. The surface is approximated by a smooth hard wall at 0 K. The CH_4 -surface interaction potential is assumed to be a square well with a binding energy of $2.9 \text{ kcal mol}^{-1}$ as experimentally determined.¹⁰ The attractive part of the Ar-surface interaction potential is neglected. The CH_4 is initially stationary at a position 1.2 \AA beyond the distance of hard-sphere-hard-wall surface contact. Energy accommodation upon the CH_4 -surface collision is modeled within the hard cube model,¹¹ assuming a surface effective mass of 88.1 amu.¹² Ar-surface collisions are taken to be completely elastic. Except for impulsive collisions with the surface and between each other, no additional exter-

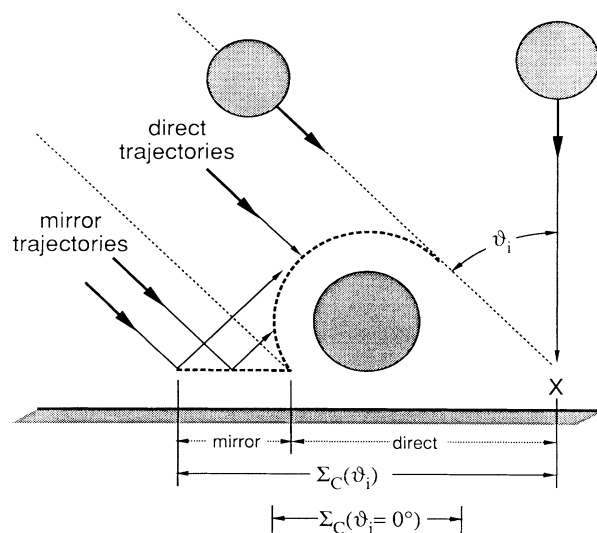


FIG. 2. Schematic diagram of collision of Ar with physisorbed CH_4 showing relative contributions of direct collisions and mirror collisions to collision cross section $\Sigma_C(\theta_i)$ at a glancing angle of incidence. The dashed line represents the closest approach of the Ar center of mass to the surface or to the physisorbed CH_4 for all glancing-angle trajectories that result in a collision. The dotted line separates trajectories at a glancing angle that lead to direct collisions from those that lead to no collisions or lead to mirror collisions. The collision cross section at normal incidence $\Sigma_C(\theta_i = 0^\circ)$ and an Ar atom incident at the normal angle but outside of the collision area is also shown.

nal force influences the normal and tangential motion of the Ar or the CH_4 . Although extremely simple, this model incorporates the essential physics of collision-induced desorption as will now be seen. The results of these calculations show the dependence of Σ_D on E_i and θ_i to be the consequence of two competing effects.

First, for desorption to occur, the physisorbed CH_4 must be hit by the incident Ar atom. The probability of collision is given by the geometric collision cross section, Σ_C , which is defined as the surface area per CH_4 inside of which an Ar atom cannot strike without colliding with CH_4 . Two types of collisions, direct and mirror collisions, contribute to Σ_C as depicted in Fig. 2. In a direct collision, the Ar hits the CH_4 on its incoming trajectory. Mirror collisions take place on the outgoing Ar trajectory after the Ar has suffered a collision with the surface. Consider the possibility of a CH_4 -Ar collision as θ_i is increased for Ar aimed at a position \times on the surface shown in Fig. 2. At $\theta_i = 0^\circ$, a collision between the Ar and CH_4 cannot occur because position \times is farther from the CH_4 molecule than a hard-sphere collision diameter. However, some larger θ_i will support a direct collision with CH_4 , thereby resulting in a larger Σ_C . Likewise, mirror collisions are not possible at $\theta_i = 0^\circ$ but become more likely as θ_i is increased. Therefore, Σ_C is a strongly increasing function of θ_i , a conclusion supported by

Σ_C calculated from the classical trajectories and shown in Fig. 3(a). The large increase in Σ_C at glancing θ_i is a direct result of the projection of the Ar-CH₄ interaction above the surface plane.¹³ This important trend is general to the cross section for collision of an incident particle with any isolated adsorbate on a smooth surface. The exact dependence of Σ_C on θ_i is an intrinsic function of the shape of the Ar-CH₄ interaction potential. Within the hard-sphere approximation, Σ_C is independent of E_i .

Upon the Ar-CH₄ collision, the efficiency of kinetic energy transfer to CH₄ motion normal to the surface determines the subsequent fate of the CH₄ with respect to desorption. The impact parameter of the Ar-CH₄ collision defines the fraction of the Ar kinetic energy transferred to CH₄. The energy transfer is maximum

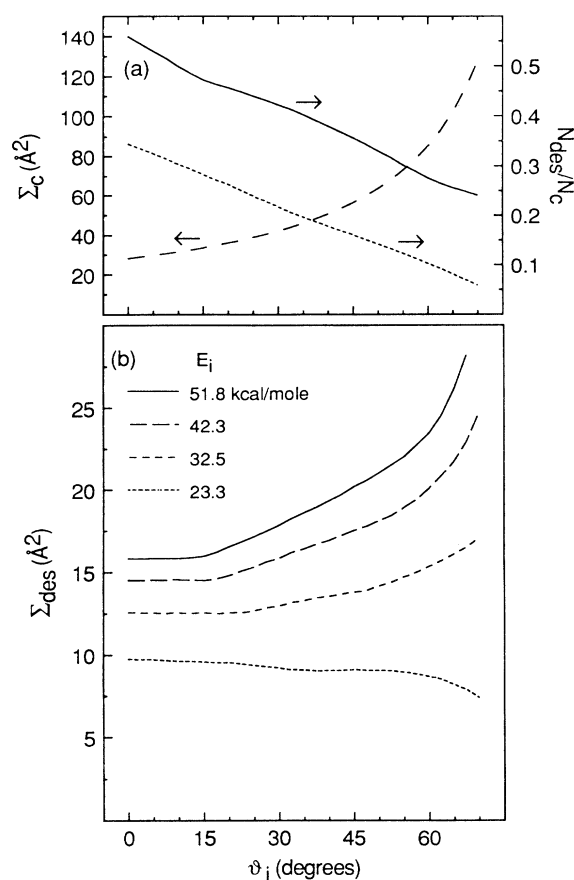


FIG. 3. Results of classical trajectory calculations as described in text. (a) Collision cross section Σ_C vs angle of incidence of Ar; fraction of collisions which yield sufficient normal energy for desorption (>2.9 kcal mol⁻¹), N_D/N_C , vs angle of incidence of Ar for total kinetic energies of 51.8 and 23.3 kcal mol⁻¹. (b) Desorption cross section Σ_D as a function of angle of incidence for several total Ar kinetic energies. The Σ_D is the product of Σ_C and the fraction of collisions which lead to desorption as shown in (a).

when the kinetic energy along the line of centers is maximum at small-impact-parameter collisions and decreases steadily with increasing impact parameter. As E_i is increased, larger-impact-parameter collisions with smaller fractional energy transfers begin to contribute to desorption so that Σ_D increases with E_i . However, for desorption to occur, the normal kinetic energy of the CH₄ after the collision must be greater than the CH₄-surface binding energy of 2.9 kcal mol⁻¹. Energy transferred to CH₄ in the tangential direction is not effective in overcoming the CH₄-surface attractive interaction normal to the surface because the CH₄-surface interaction potential is not sufficiently corrugated to couple tangential energy to normal energy. The fraction of Ar kinetic energy that can be transferred to CH₄ normal kinetic energy decreases as θ_i increases, thereby decreasing the fraction of collisions which result in CH₄ having sufficient kinetic energy in the normal direction to desorb. The calculated fraction of collisions which result in desorption, N_D/N_C , is plotted in Fig. 3(a) as a function of θ_i for a high (51.8 kcal mol⁻¹) and low (23.3 kcal mol⁻¹) total energy. For the small-impact-parameter collisions which are most effective at transferring energy, the smaller magnitude of the normal energy available for transfer at low energy is primarily responsible for the smaller fraction of desorbing collisions.

The decrease in the fraction of collisions with sufficient normal energy to desorb counters the increase in Σ_C and is the source of the complex dependence of Σ_D on E_i and θ_i . The desorption cross section is the product of the fraction of desorbing collisions and Σ_C and is shown in Fig. 3(b). At 51.8 kcal mol⁻¹, the angular dependence of Σ_D is similar to that of Σ_C as can be seen from the data shown in Fig. 1 and from the calculations shown in Fig. 3. At 23.3 kcal mol⁻¹, the very small fraction of desorbing collisions at glancing θ_i moderates the increase in Σ_C , resulting in the approximate independence of Σ_D on θ_i . Therefore, the competition between the increase in Σ_C and the decrease in the energy transferred to CH₄ motion in the normal direction with increasing θ_i is responsible for the major trends in Σ_D . The good qualitative agreement between the behavior of the desorption cross section determined experimentally and that calculated from the classical trajectories provides further support for the conclusion that desorption results mainly from a direct and impulsive, bimolecular collision.

We have also investigated the roles of CH₄-surface and Ar-surface energy accommodation, quenching of the transferred energy by multiple Ar-CH₄ collisions, the initial distance of CH₄ from the surface, and the attractive part of the Ar-surface interaction potential on the collision-induced desorption process.¹⁰ However, these physically real effects modify only the magnitudes of the calculated Σ_D and not the essential principles established here for collision-induced desorption. In particular, multiple collisions do not play a significant role because the

barrier to motion of physisorbed CH₄ tangential to the smooth surface is very small. A detailed quantitative comparison of the calculated and experimental cross sections and analysis of these additional effects follows in a full manuscript.¹⁰

In summary, we have shown that collision-induced desorption near the threshold energy for desorption occurs as a result of a direct and impulsive, bimolecular collision of the incident particle with the adsorbate. The collision cross section and normal energy transfer upon a single collision are the two sole important components in determining the dependences of the cross section for collision-induced desorption on energy and incident angle. The knowledge that desorption of an adsorbate can be induced by collision with a low-energy, incident atom now makes it necessary to assess the importance of collision-induced desorption along with collision-induced dissociation⁹ as a potential major step in the mechanism of any surface process, such as heterogeneous catalysis, chemical vapor deposition, and etching, occurring under significant pressure of ambient gas.

This work is supported by the NSF (Grant No. CHE-8508734), Synthetic Fuels Center of the MIT Energy Lab, and Petroleum Research Fund. S.T.C. would like to thank the Alfred P. Sloan Foundation and the Camille and Henry Dreyfus Foundation for financial support.

^(a)To whom correspondence should be addressed.

¹B. J. Garrison and N. Winograd, *Science* **216**, 805 (1982).

²An exception to this statement may be some early work by W. J. Hays, W. E. Rogers, and E. L. Knuth, *J. Chem. Phys.* **56**, 1652 (1972), who attributed the decreased width of a specularly scattered He beam to the sputtering of adsorbed contaminants by a molecular beam of Ar with a kinetic energy greater than 4 eV.

³Y. Zeiri, J. J. Low, and W. A. Goddard, III, *J. Chem. Phys.* **84**, 2408 (1986).

⁴S. L. Tang, J. D. Beckerle, M. B. Lee, and S. T. Ceyer, *J. Chem. Phys.* **84**, 6488 (1986).

⁵M. B. Lee, Q. Y. Yang, and S. T. Ceyer, *J. Chem. Phys.* **87**, 2724 (1987).

⁶S. T. Ceyer, J. D. Beckerle, M. B. Lee, S. L. Tang, Q. Y. Yang, and M. A. Hines, *J. Vac. Sci. Technol. A* **5**, 501 (1987).

⁷S. T. Ceyer, *Annu. Rev. Phys. Chem.* **39**, 479 (1988).

⁸J. D. Beckerle, Q. Y. Yang, A. D. Johnson, and S. T. Ceyer, *Surf. Sci.* **195**, 77 (1988).

⁹J. D. Beckerle, Q. Y. Yang, A. D. Johnson, and S. T. Ceyer, *J. Chem. Phys.* **86**, 7236 (1987).

¹⁰J. D. Beckerle, A. D. Johnson, and S. T. Ceyer, to be published.

¹¹R. M. Logan and R. E. Stickney, *J. Chem. Phys.* **44**, 195 (1966).

¹²E. K. Grimmelmann, J. C. Tully, and M. J. Cardillo, *J. Chem. Phys.* **72**, 1039 (1980).

¹³B. Poelsema, R. L. Palmer, S. T. de Zwart, and G. Comsa, *Surf. Sci.* **126**, 641 (1983).